

Sampling for the V-line Transform with Vertex in a Circle

Duy N. Nguyen* and Linh V. Nguyen†

August 25, 2020

Abstract

In this paper, we consider a special V-line transform. It integrates a given function f over the V-lines whose centers are on a circle centered at the origin and the symmetric axes pass through the origin. We derive two sampling scheme of the transform: the standard and interlaced ones. We prove the an error estimate for the schemes, which is explicitly expressed in term of f .

1 Introduction

The V-line transform arises in Compton camera imaging. Let us first recall the classical setup single-photon emission computed tomography SPECT, which is a nuclear medicine tomographic imaging technique using gamma rays. In SPECT, weakly radioactive tracers are given to the patient. The radioactive tracers can be detected through the emission of gamma ray photons revealing the information about biochemical processes. Then one uses a gamma camera to record photons that enter the detector surface perpendicularly. That is, the camera measures the integrals of the tracer distribution over straight lines that are orthogonal to its surface, see Fig 1.

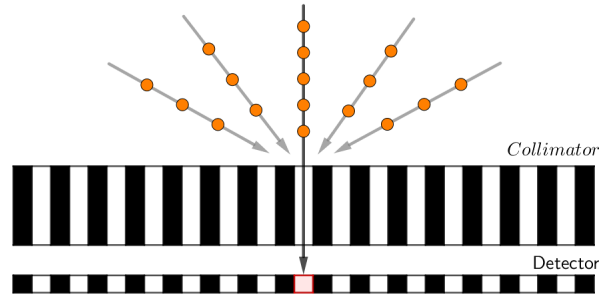


Figure 1: Gamma camera for SPECT. Only orthogonal photons measured in detector, other is removed.

This technique removes most photons and only a few photons are recorded. Therefore, a new type of camera for SPECT, which makes use of Compton scattering, was proposed by Everett [6] and Singh [27]. It uses electronic collimation as an alternative to mechanical collimation, which provides both high efficiency and multiple projections of the object. The camera consists of two plane gamma detectors positioned one behind the other. An emitted photon undergoes Compton scattering in the first detector surface D_1 and is absorbed by the second detector surface D_2 . In each detector surface, the position and the energy of the photon are measured. The scattering angle at D_1 is determined via the Compton scattering formula $\cos \psi = 1 - \frac{mc^2(E_1 E_2)}{E_1 E_2}$, where m is the electron mass, c the speed of light, E_1 the photon energy at D_1 ,

*High School for the Gifted, Ho Chi Minh City, Vietnam. Email: nnduy@ptnk.edu.vn.

†University of Idaho, 875 Perimeter Dr, Moscow, ID 83844, USA. Email: lnguyen@uidaho.edu.

and E_2 the energy of the photon measured at D_2 . So a photon observed at $x_1 \in D_1$ and $x_2 \in D_2$ with the energy E_1, E_2 respectively must have been emitted on the surface of the circular cone, whose vertex is at x_1 , central axis points from x_2 to x_1 , and the half-opening angle is given by ψ (see Fig. 2).

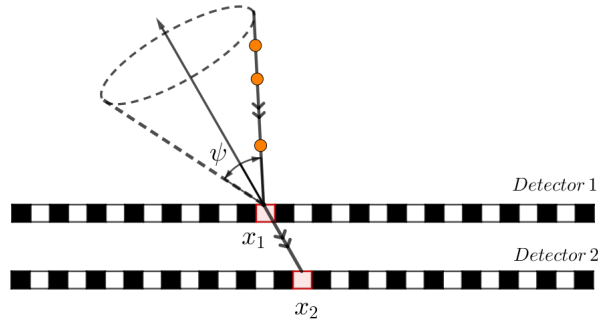


Figure 2: Compton camera

As a result, a Compton camera gives us the integrals of emission distribution on conical surfaces whose vertices are on the D_1 . The mathematical problem of **Compton camera imaging** is to reconstruct the emission distribution from such integrals.

There are quite a few works on the mathematical problems of Compton camera. Specially in the two dimensional space, the cone become V-line and there exist some inversion formulas (e.g. [4, 23, 30]). In the three dimensional space, the space of conical surfaces whose vertices are on a detector surface is a five dimensional manifold. One is in the situation of redundant data. Taking advantage of such redundancy was the topic of several works (see, e.g.,[16]). One, however, may wish to restrict themselves into the lower dimensional data. In this article, we are interested in the sampling theory for Compton camera imaging in two dimensional space (i.e., the V-line transform).

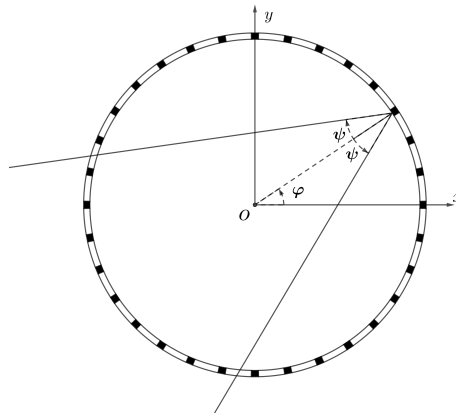


Figure 3: Our setups: the V-line transform over all V-lines whose vertices are on the circle of radius r centered at the origin and whose symmetric axis pass through the origin.

Namely, let f be a b -essentially band-limited function supported in the circle of radius $r_0 \leq 1$ centered at the origin. We consider the V-line transform $V(f)$ of f on all the V-lines whose vertex is on the circle of radius $r > 1$ centered at the origin and the symmetric axis passing through the origin, see Fig. 3.

Definition 1.1. Let f be a compactly supported function in $D_1(0)$. The V-line transform $Vf(\varphi, \psi)$ of f is defined by

$$Vf : [0, 2\pi) \times (0; \pi) \longrightarrow \mathbb{R},$$

$$(\varphi, \psi) \longmapsto \sum_{\sigma=\pm 1} \int_0^{+\infty} f(r\theta(\varphi) - t\theta(\varphi + \sigma\psi)) dt.$$

We consider the problem of recovering function Vf from its discrete measures $Vf(\varphi_k, \alpha_m)$. That is, we consider efficient sampling schemes to recover the V-line transform. Using Shannon sampling series and classical Fourier analysis, several authors [7, 8, 10, 18] study the reconstruction of the standard Radon and circular Radon transforms from its discrete measurement. More recently, Stefanov [28] employed semi-classical analysis to study the same problem for generalized Radon transform.

In this work, we introduce two sampling schemes. The first one is the standard sampling scheme, which is $(\varphi, \psi) = (\varphi_k, \psi_m)$, $0 \leq k \leq N_\varphi - 1, 0 \leq m \leq N_\psi - 1$. Here, φ_k and ψ_m are evenly spaced in their domains. By restricting on the cones that intersect with the support of f , we only consider

$$\varphi_k = \frac{k2\pi}{N_\varphi}, \quad \text{for } 0 \leq k \leq N_\varphi - 1,$$

$$\psi_m = \frac{m2\pi}{N_\psi}, \quad \text{for } 0 \leq m < \frac{N_\psi \arcsin(r_0/r)}{2\pi}.$$

To well recover g from the discrete data we need

$$N_\varphi \geq 2\pi rb, \quad N_\psi \geq 4rb.$$

The total number M_0 of needed samples has to satisfy

$$M_0 \geq 4(rb)^2 \arcsin(r_0/r).$$

The second, more efficient, sampling scheme is given by

$$\varphi_k = \frac{k2\pi}{N_\varphi} \quad \text{for } 0 \leq k \leq N_\varphi - 1,$$

$$\psi_{k,m} = \frac{\pi m}{N_\psi} \quad \text{for } k, m \text{ are parity and } 0 \leq m < \frac{N_\psi \arcsin(r_0/r)}{\pi},$$

with the sampling conditions

$$N_\varphi \geq 2\pi rb, \quad N_\psi \geq 3rb.$$

The total number of samples satisfies

$$M_0 \geq 3(rb)^2 \arcsin(r_0/r),$$

which is three quarters of the standard scheme.

The article is organized as follows. In Section 2, we introduce some preliminaries.

2 Preliminaries

The 2D Radon transform. We recall the 2D Radon transform that maps a function f on \mathbb{R}^2 into the set of its integrals over the lines on \mathbb{R}^2 . If $\theta(\varphi) = (\cos \varphi, \sin \varphi) \in S^1$ is a unit vector and s is a real number. The Radon transform $Rf(\varphi, s)$ is defined as

$$Rf(\varphi, s) = \int_{x \cdot \theta = s} f(x) dl = \int_{-\infty}^{+\infty} f(s \cos \varphi - t \sin \varphi; s \sin \varphi + t \cos \varphi) dt.$$

In this notation, $Rf(\varphi, s)$ is the integral of f over the line with a normal direction θ and of the distance s from the origin. Let $R_\varphi f(\cdot) = Rf(\varphi, \cdot)$, a useful relation between the 1D Fourier transform of $R_\varphi f$ and the 2D Fourier transform of f is as follows

$$(R_\varphi f)^\wedge(\sigma) = (2\pi)^{1/2} \hat{f}(\sigma \cdot \theta).$$

Here, the Fourier transform of a function g defined on \mathbb{R}^n is given by

$$\hat{g}(\xi) = \frac{1}{(2\pi)^{n/2}} \int_{\mathbb{R}^n} g(x) e^{-ix \cdot \xi} dx.$$

The inversion formula of 2D Radon transform is

$$f(x, y) = \frac{-1}{4\pi^2} \int_0^\pi \int_{-\infty}^{+\infty} \frac{\frac{\partial}{\partial s} Rf(\varphi, s)}{s - x \cos \varphi - y \sin \varphi} ds d\varphi.$$

One can see the following relationship between V-line transform and Radon transform

$$Vf(\varphi, \psi) = Rf\left(\varphi + \psi - \frac{\pi}{2}, r \sin \psi\right) + Rf\left(\varphi - \psi - \frac{\pi}{2}, -r \sin \psi\right).$$

Sampling of periodic functions. Let g be a function in \mathbb{R}^n that is periodic with respect to n vectors p_1, p_2, \dots, p_n . If the matrix $P = (p_1, p_2, \dots, p_n)$ is nonsingular then g is called a P-periodic function. One denotes $L_P = P\mathbb{Z}^n$ and its reciprocal lattice $L_P^\perp = L_{2\pi P^{-T}}$. We define the discrete Fourier transform of g be the following function on L_P^\perp :

$$\hat{g}(\xi) = |\det(P)|^{-1} \int_{P[0,1]^n} g(x) e^{-ix \cdot \xi} dx, \quad \xi \in L_P^\perp.$$

Let us note that g can be recovered from its Fourier coefficients by the series [29]

$$g(x) = \sum_{\xi \in L_P^\perp} \hat{g}(\xi) e^{ix \cdot \xi}.$$

Let W be a real nonsingular $n \times n$ -matrix, our goal is study the sampling of g on L_W . For this to make, we assume $L_P \subset L_W$. This case is implied if and only if $P = WM$ with an integer matrix M . Hence, $L_W^\perp \subset L_P^\perp$. Our study relies heavily on Poisson summation formula for a P-periodic function g , see [8]. It reads

$$\sum_{y \in L_W/L_P} g(x+y) = \left| \frac{\det(P)}{\det(W)} \right| \sum_{\xi \in L_W^\perp} \hat{g}(\xi) e^{ix \cdot \xi}.$$

Here, L_W/L_P is the quotient space whose elements are of the form $y + L_P$. In particular, using the Poisson summation formula one obtains (see [7, 11])

Theorem 2.1. *Suppose $g \in C^\infty(\mathbb{R}^n)$ is a P-periodic function. Let $K \subset L_P^\perp$ be a finite set such that its translates $K + \eta$, $\eta \in L_W^\perp$ are disjoint, and χ_K denotes the characteristic function of K , i.e., $\chi_K(\xi) = 1$ if $\xi \in K$ and $\chi_K(\xi) = 0$ otherwise. We define the sampling series*

$$S_{W,K}g(x) := \left| \frac{\det W}{\det P} \right| \sum_{v \in L_W/L_P} \widetilde{\chi}_K(x-v) g(v).$$

Then,

$$\|S_{W,K}g - g\|_{L^\infty} \leq 2 \int_{L_P^\perp \setminus K} |\hat{g}(\xi)| d\xi.$$

Sampling of the V-Line transform. Because of $\text{supp}(f) \subset D_1(0)$, so that $Vf(\varphi, \psi) = 0$ with $\psi \in \left[\frac{\pi}{2}, \pi\right)$. Consequently, Vf can expand to an even function in ψ variable and 2π -periodic in both variables. We will make use of the two dimension form of Theorem 2.1 to recover the V-line transform. For $f \in C^\infty(D_1(0))$, we denote $g(\varphi, \psi) = Vf(\varphi, \psi)$. Since, g is 2π -periodic in each variables, then the periodic matrix of g is $P = 2\pi I_{2 \times 2}$ and $L_P^\perp = \mathbb{Z}^2$. We chose matrix W which satisfies the condition $L_P \subset L_W$ as

$$W = 2\pi \begin{pmatrix} 1/P & 0 \\ N/(PQ) & 1/Q \end{pmatrix}$$

where P, Q, N are three integers such that $P, Q > 0$ and $0 \leq N < P$. Therefor,

$$L_W/L_P = \{(s_j, t_{jl}) : s_j = \frac{j2\pi}{P}, t_{jl} = \frac{(l + Nj/P)2\pi}{Q}, j = 0, \dots, P-1, l = 0, \dots, Q-1\}.$$

The sampling theorem for this setting follows as

Theorem 2.2. *Suppose $f \in C_0^\infty(D_1(0))$ and $g(\varphi, \psi) = Vf(\varphi, \psi)$. Let $K \subset \mathbb{Z}^2$ be a finite set such that its translates $K + \eta$, $\eta \in L_W^\perp$ are disjoint. For $x \in [0, 2\pi) \times [0, 2\pi)$, the sampling series is*

$$S_{W,K}g(x) := \frac{1}{PQ} \sum_{v \in L_W/L_P} \widetilde{\chi}_K(x-v)g(v).$$

Then,

$$\|S_{W,K}g - g\|_{L^\infty} \leq 2 \sum_{\mathbb{Z}^2 \setminus K} |\widehat{g}(\xi)| d\xi.$$

3 The main results

Our goal is to use the Theorem 2.2 to propose some sampling conditions and derive a corresponding sampling error estimate. For this purpose, we assume $\widehat{f}(\xi)$ be negligible for $|\xi| > b$, in the sense that the integral $\epsilon_d(f, b) := \int_{|\xi| > b} |\xi|^d |\widehat{f}(\xi)| d\xi$ is small for all real number d . Such a function f is called essentially b -band-limited. Here is the main result of this article:

Theorem 3.1. *Let $f \in C_0^\infty(D)$ be essentially b -band-limited ($b > 1$), and $g(\varphi, \psi) = Vf(\varphi, \psi)$. Let $\vartheta < 1$ be such that $2 - \vartheta^2 < r$. We define the set*

$$K = \left\{ (k, m) : |k| < \frac{rb}{\vartheta}; \max\{|k+m|, |k-m|\} < rb \right\}$$

in \mathbb{R}^2 . Let W be a real non-singular 2×2 matrix such that the sets $K + 2\pi(W^{-1})l$, $l \in \mathbb{Z}^2$ are mutually disjoint.

Let

$$\begin{aligned} \eta_1(\vartheta, \gamma) &= \left(\frac{3}{(1-\vartheta^2)^{3/2}} + \frac{9}{(1-\vartheta^2)^3} \frac{1}{\gamma} \right) \eta(\vartheta, \gamma), \\ \eta_2(\vartheta, \gamma) &= \left(\frac{9}{(1-\vartheta^2)^3} + \frac{54}{(1-\vartheta^2)^{9/2}} \frac{1}{\gamma} \right) \eta(\vartheta, \gamma), \\ \eta_3(\vartheta, \gamma) &= \gamma \eta_1(\vartheta, \gamma) + \eta_2(\vartheta, \gamma), \end{aligned}$$

where $\eta(\vartheta, \gamma) = \gamma \vartheta \exp(-\frac{\gamma}{3}(1-\vartheta^2)^{3/2})$. Then for b being big enough

$$\|S_{W,K}g - g\|_{L^\infty} \leq \frac{12}{\pi} \eta^*(\vartheta, rb) \|f\|_{L^1(\mathbb{R}^2)} + \frac{4r^2}{\pi \vartheta^3} (2b+1) \epsilon_1(f, b),$$

where $\eta^*(\vartheta, \gamma) = \max \left\{ \frac{2b}{\vartheta^2} \eta_1\left(\vartheta, \frac{\gamma}{\vartheta}\right); \frac{1}{r} \eta_2\left(\vartheta, \frac{\gamma}{\vartheta}\right); \frac{\vartheta}{r^2 - \vartheta^2} \eta_3\left(\vartheta, \frac{\gamma}{\vartheta^2}\right) \right\}$.

In the rest of this article, we present the proof of this theorem. We then discuss two related sampling schemes.

3.1 Proof of the main result

We first derive some useful property of Fourier coefficient of V-line transform (see [7]).

Lemma 3.2. *Suppose $f \in C_0^\infty(D_1(0))$, $g(\varphi, \psi) = Vf(\varphi, \psi)$. Let $\widehat{g}_{k,m}$ be the Fourier coefficient of g . Then*

$$\widehat{g}_{k,m} = \frac{i^k}{2\pi} \int_{\mathbb{R}} \int_0^{2\pi} \widehat{f}(\sigma\theta(\alpha)) [J_{k-m}(\sigma) + J_{k+m}(\sigma)] e^{-ik\alpha} d\alpha d\sigma,$$

with $J_k(x)$ is Bessel function of first kind.

Proof. We have

$$\begin{aligned} \widehat{g}_{k,m} &= \frac{1}{4\pi^2} \int_0^{2\pi} \int_{-\pi}^{\pi} g(\varphi, \psi) e^{-i(k\varphi+m\psi)} d\varphi d\psi \\ &= \frac{1}{4\pi^2} \int_0^{2\pi} \int_{-\frac{\pi}{2}}^{\frac{\pi}{2}} \left[Rf\left(\varphi + \psi - \frac{\pi}{2}, r\theta\left(\varphi + \psi - \frac{\pi}{2}\right)\theta(\varphi)\right) + Rf\left(\varphi - \psi - \frac{\pi}{2}, r\theta\left(\varphi - \psi - \frac{\pi}{2}\right)\theta(\varphi)\right) \right] \times \\ &\quad e^{-i(k\varphi+m\psi)} d\varphi d\psi \\ &= I_1 + I_2, \end{aligned}$$

where

$$I_{1,2} = \int_0^{2\pi} \int_{-\frac{\pi}{2}}^{\frac{\pi}{2}} Rf\left(\varphi + \psi - \frac{\pi}{2}, r\theta\left(\varphi \pm \psi - \frac{\pi}{2}\right)\theta(\varphi)\right) e^{-im\psi} d\varphi d\psi.$$

Changing variable $\alpha = \varphi + \psi - \frac{\pi}{2}$, the integral inside of I_1 becomes

$$\begin{aligned} &\int_{-\frac{\pi}{2}}^{\frac{\pi}{2}} Rf\left(\varphi + \psi - \frac{\pi}{2}, r\theta\left(\varphi + \psi - \frac{\pi}{2}\right)\theta(\varphi)\right) e^{-im\psi} d\psi \\ &= (-i)^k \int_{\varphi-\pi}^{\varphi} Rf[\alpha, r\theta(\alpha)\theta(\varphi)] e^{-im\alpha} e^{im\varphi} d\alpha \\ &= \frac{(-i)^k}{2} e^{im\varphi} \int_0^{2\pi} Rf[\alpha, r\theta(\alpha)\theta(\varphi)] e^{-im\alpha} d\alpha \\ &= \frac{(-i)^k}{2\sqrt{2\pi}} e^{im\varphi} \int_0^{2\pi} \left(\int_{\mathbb{R}} (Rf)(\alpha, \sigma) e^{ir\theta(\alpha)\theta(\varphi)\sigma} d\sigma \right) e^{-im\alpha} d\alpha \\ &= \frac{(-i)^k}{2} e^{im\varphi} \int_0^{2\pi} \int_{\mathbb{R}} \widehat{f}(\sigma\theta(\alpha)) e^{-im\alpha + ir\sigma \cos(\varphi-\alpha)} d\sigma d\alpha. \end{aligned}$$

Hence,

$$\begin{aligned} I_1 &= \frac{(-i)^k}{8\pi^2} \int_0^{2\pi} \int_{\mathbb{R}} \widehat{f}(\sigma\theta(\alpha)) \int_0^{2\pi} e^{-i(k-m)\varphi} e^{-im\alpha + ir\sigma \cos(\varphi-\alpha)} d\varphi d\sigma d\alpha \\ &= \frac{(-i)^k}{8\pi^2} \int_0^{2\pi} \int_{\mathbb{R}} \widehat{f}(\sigma\theta(\alpha)) e^{-ik\alpha} \left(\int_0^{2\pi} e^{-i(k-m)(\varphi-\alpha) + ir\sigma \cos(\varphi-\alpha)} d\varphi \right) d\alpha d\sigma. \end{aligned}$$

Noting that

$$J_k(x) = \frac{i^{-k}}{2\pi} \int_0^{2\pi} e^{ix \cos \varphi - ik\varphi} d\varphi,$$

we obtain

$$I_1 = \frac{i^k}{4\pi} \int_0^{2\pi} \int_{\mathbb{R}} \widehat{f}(\sigma\theta(\alpha)) e^{-ik\alpha} J_{k-m}(r\sigma) d\alpha d\sigma. \quad (1)$$

Similarly,

$$I_2 = \frac{i^k}{4\pi} \int_0^{2\pi} \int_{\mathbb{R}} \widehat{f}(\sigma\theta(\alpha)) e^{-ik\alpha} J_{k+m}(r\sigma) d\alpha d\sigma. \quad (2)$$

Combining (1) and (2), we conclude

$$\widehat{g}_{k,m} = \frac{i^k}{4\pi} \int_0^{2\pi} \int_{\mathbb{R}} \widehat{f}(\sigma\theta(\alpha)) [J_{k-m}(r\sigma) + J_{k+m}(r\sigma)] e^{-ik\alpha} d\alpha d\sigma.$$

□

In order to estimate $\widehat{g}_{m,k}$ we will need the following result

Lemma 3.3. *Suppose $f \in C_0^\infty(D_1(0))$, $g(\varphi, \psi) = Vf(\varphi, \psi)$. Let $\widehat{g}_{k,m}$ be the Fourier coefficient of g . Then*

$$\left| \int_{\mathbb{R}} \int_0^{2\pi} \widehat{f}(\sigma\theta(\alpha)) J_l(\sigma) e^{-ik\alpha} d\alpha d\sigma \right| \leq \int_{D_1(0)} |f(x)| \left| \int_{-\sigma}^{\sigma} J_l(r\sigma) J_k(\sigma|x|) d\sigma \right| dx + 2\epsilon_{-1}(f, \sigma),$$

Proof. Since the Bessel function is bounded by 1,

$$\left| \int_{\mathbb{R}} \int_0^{2\pi} \widehat{f}(\sigma\theta(\alpha)) J_l(\sigma) e^{-ik\alpha} d\alpha d\sigma \right| \leq \frac{1}{4\pi} \left| \int_{-\sigma}^{\sigma} \int_0^{2\pi} \widehat{f}(\sigma\theta) e^{-ik\alpha} J_l(r\sigma) d\alpha d\sigma \right| + \frac{1}{2\pi} \epsilon_{-1}(f, \sigma).$$

Expressing $\widehat{f}(\sigma\theta)$ by its definition, we obtain

$$\begin{aligned} \int_0^{2\pi} \widehat{f}(\sigma\theta(\alpha)) e^{-ik\alpha} d\alpha &= \frac{1}{2\pi} \int_0^{2\pi} \int_{D_1(0)} f(x) e^{-i\sigma\theta x} e^{-ik\alpha} dx d\alpha \\ &= \frac{1}{2\pi} \int_{D_1(0)} f(x) \int_0^{2\pi} e^{-i(\alpha|x| \cos(\alpha-\psi) + k(\alpha-\psi))} e^{-ik\psi} d\alpha dx \\ &= \int_{D_1(0)} f(x) J_k(-\sigma|x|) dx. \end{aligned}$$

This gives us the desired in equality.

□

The following inequality in [26]

$$J_\nu(vs) \leq \frac{s^\nu \exp(v(1-s^2)^{1/2})}{(1+(1-s^2))^{1/2}}, \quad v \geq 0, \quad 0 < s \leq 1,$$

yields

$$J_\nu(vs) \leq e^{-\frac{s}{3}(1-s^2)^{3/2}}, \quad v \geq 0, \quad 0 < s \leq 1.$$

We obtain

$$\sup_{|x| \leq 1} \int_{-\vartheta k}^{\vartheta k} |J_k(\sigma|x|)| d\sigma \leq 2k\vartheta \sup_{|x| \leq 1} \int_0^1 J_k(k\sigma\vartheta|x|) d\sigma \leq 2k\vartheta \int_0^1 e^{-\frac{\gamma}{3}(1-|\vartheta\sigma|^2)^{3/2}} d\sigma \leq 2\eta(\vartheta, \gamma), \quad (3)$$

where

$$\eta(\vartheta, \gamma) = k\vartheta \exp\left(-\frac{\gamma}{3}(1-\vartheta^2)^{3/2}\right).$$

Lemma 3.4. *Assume that $|k| < \vartheta^{-1}|l|$. Choosing $\sigma = \vartheta|l|$, then the following holds.*

$$\int_{D_1(0)} |f(x)| \left| \int_{-\sigma}^{\sigma} J_l(r\sigma) J_k(\sigma|x|) d\sigma \right| dx \leq 2\eta(\vartheta, |l|) \|f\|_{L^1(\mathbb{R}^2)}.$$

Proof. Indeed, using the fact that $|J_k(s)| \leq 1$ for all $s \geq 1$, we obtain

$$\begin{aligned} \int_{D_1(0)} |f(x)| \left| \int_{-\sigma}^{\sigma} J_l(r\sigma) J_k(\sigma|x|) d\sigma \right| dx &\leq \left(\int_{|\sigma| \leq \vartheta|l|/r} |J_l(r\sigma)| d\sigma \right) \|f\|_{L^1(\mathbb{R}^2)} \\ &\leq \left(\frac{1}{r} \int_{|\sigma| \leq \vartheta|l|} |J_l(\sigma)| d\sigma \right) \|f\|_{L^1(\mathbb{R}^2)} \\ &\stackrel{(3)}{\leq} \frac{2}{r} \eta(\vartheta, |l|) \|f\|_{L^1(\mathbb{R}^2)}. \end{aligned}$$

□

We will also need the following result

Lemma 3.5. *Suppose $f \in C_0^\infty(D_1(0))$ and $\bar{r} := 2 - \vartheta^2 < r$, then for $|k| \geq \vartheta^{-1}|l|$,*

$$\left| \int_{\mathbb{R}} \int_0^{2\pi} \widehat{f}(\sigma\theta(\alpha)) J_l(\sigma) e^{-ik\alpha} d\alpha d\sigma \right| \leq \frac{1}{2\pi(r^2 - \bar{r}^2)k\vartheta} \eta(k, \vartheta) \|f\|_{L^1(\mathbb{R}^2)}.$$

Proof. From [13], for any positive real number ϵ such that $\rho := \sqrt{\cosh 2\epsilon} \leq r$, we have

$$\left| \int_{\mathbb{R}} \int_0^{2\pi} \widehat{f}(\sigma\theta(\alpha)) J_l(\sigma) e^{-ik\alpha} d\alpha d\sigma \right| \leq \frac{I(f)}{2\pi} \exp\left(-\epsilon|k| + \frac{\delta}{r}|l|\right)$$

where $\delta := \int_0^\epsilon \sqrt{\cosh 2t} dt$ and

$$I(f) := \int_{D_1(0)} \frac{|f(x, y)|}{r^2 - \bar{r}^2(x^2 + y^2)} dx dy.$$

Simple calculation give for for all $\epsilon < 1$,

$$\delta = \int_0^\epsilon \sqrt{\cosh 2t} dt \leq \epsilon \sqrt{\cosh 2\epsilon} < \epsilon(1 + \epsilon).$$

Choosing $\epsilon = (1 - \vartheta^2)$ we obtain

$$\epsilon - \frac{\delta\vartheta}{r} \geq \epsilon(1 - \frac{1+\epsilon}{r}\vartheta) \geq \epsilon(1 - \vartheta) \geq \epsilon(1 - \sqrt{1-\epsilon}) \geq \frac{1}{3}\epsilon^{3/2} = (1 - \vartheta^2)^{3/2}$$

Therefore, for $|k| \geq \vartheta^{-1}|l|$,

$$\exp\left(-\epsilon|k| + \frac{\delta}{r}|l|\right) \leq \exp\left(-\frac{|k|}{3}(1 - \vartheta^2)^{3/2}\right).$$

Moreover, since $\rho = \cosh(2\epsilon) < 1 + \epsilon = \bar{r}$,

$$I(f) := \int_{D_1(0)} \frac{|f(x, y)|}{r^2 - \bar{r}^2(x^2 + y^2)} dx dy \leq \frac{1}{r^2 - \bar{r}^2} \|f\|_{L^1(\mathbb{R}^2)}.$$

The above two inequalities finish our proof. □

We are now ready to prove Theorem 3.1.

Proof of Theorem 3.1. Due to Theorem 2.2 for the solution, suffices to prove that

$$2 \sum_{\mathbb{Z}^2 \setminus K} |\widehat{g}_{k,m}| \leq \frac{12}{\pi} \eta^*(\vartheta, rb) \|f\|_{L^1(\mathbb{R}^2)} + \frac{4r^2}{\pi\vartheta^3} (2b+1) \epsilon_1(f, b).$$

Indeed, from Lemma 3.2, we obtain

$$|\widehat{g}_{k,m}| \leq \frac{1}{2\pi} \left| \int_{\mathbb{R}} \int_0^{2\pi} \widehat{f}(\sigma\theta(\alpha)) J_{k-m}(\sigma) e^{-ik\alpha} d\alpha d\sigma \right| + \frac{1}{2\pi} \left| \int_{\mathbb{R}} \int_0^{2\pi} \widehat{f}(\sigma\theta(\alpha)) J_{k+m}(\sigma) e^{-ik\alpha} d\alpha d\sigma \right|.$$

Therefore,

$$\sum_{\mathbb{Z}^2 \setminus K} |\widehat{g}_{k,m}| \leq S_1 + S_2,$$

where

$$S_{1,2} = \sum_{\mathbb{Z}^2 \setminus K} \frac{1}{2\pi} \left| \int_{\mathbb{R}} \int_0^{2\pi} \widehat{f}(\sigma\theta(\alpha)) J_{k\mp m}(\sigma) e^{-ik\alpha} d\alpha d\sigma \right|.$$

Let us denote

$$\bar{\eta}_1(\vartheta, \gamma) = \sum_{m>k} \eta(\vartheta, m), \quad \bar{\eta}_2(\vartheta, \gamma) = \sum_{m>k} \bar{\eta}_1(\vartheta, m), \quad \bar{\eta}_3(\vartheta, \gamma) = \sum_{m>k} m\eta(\vartheta, m),$$

We note that $\eta(\vartheta, \gamma)$ exponentially decays as $k \rightarrow \infty$ and

$$\sum_{m>k} m^d \eta(\vartheta, m) \leq \int_k^\infty s^d \eta(\vartheta, s) = \int_k^\infty \vartheta s^{d+1} \exp\left(-\frac{s}{3}(1-\vartheta^2)^{3/2}\right) ds,$$

for $d \geq -1$ and k big enough. Direct calculations then show

$$\bar{\eta}_1(\vartheta, \gamma) \leq \left(\frac{3}{(1-\vartheta^2)^{3/2}} + \frac{9}{(1-\vartheta^2)^3} \frac{1}{\gamma} \right) \eta(\vartheta, \gamma) = \eta_1(\vartheta, \gamma), \tag{4}$$

$$\bar{\eta}_2(\vartheta, \gamma) \leq \left(\frac{9}{(1-\vartheta^2)^3} + \frac{54}{(1-\vartheta^2)^{9/2}} \frac{1}{\gamma} \right) \eta(\vartheta, \gamma) = \eta_2(\vartheta, \gamma), \tag{5}$$

$$\bar{\eta}_3(\vartheta, \gamma) \leq \gamma \bar{\eta}_1(\vartheta, \gamma) + \bar{\eta}_2(\vartheta, \gamma) = \eta_3(\vartheta, \gamma). \tag{6}$$

PART 1: Estimate S_1

We decompose $S_1 = S_{11} + S_{12} + S_{13}$ where each S_{ij} is the sum ranging over the region Σ_{ij} , where

$$\Sigma_{11} : = \left\{ (k, m) \in \mathbb{Z}^2 : |k| < \frac{rb}{\vartheta^2}; |k-m| \geq \frac{rb}{\vartheta} \right\},$$

$$\Sigma_{12} : = \left\{ (k, m) \in \mathbb{Z}^2 : |k| \geq \frac{rb}{\vartheta^2}; |k| > \frac{|k-m|}{\vartheta} \right\},$$

$$\Sigma_{13} : = \left\{ (k, m) \in \mathbb{Z}^2 : |k| \geq \frac{rb}{\vartheta^2}; |k| \leq \frac{|k-m|}{\vartheta} \right\}.$$

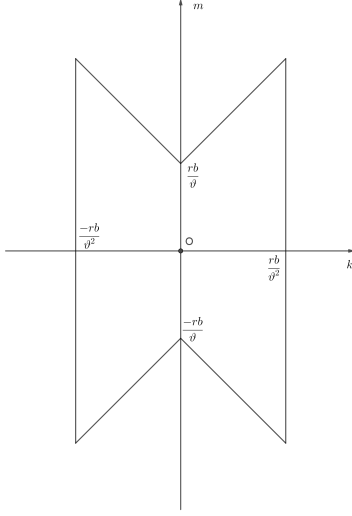


Figure 4: The set K for $\vartheta = \frac{5}{6}, b = 5, r = \frac{3}{2}$.

- For the sum S_{11} , we note that $|k - m| \geq \vartheta|k|$ in Σ_{11} . Using Lemma 3.3 and Lemma 3.4, we obtain

$$\begin{aligned}
\Sigma_{11} &\leq \sum_{|k| \leq \frac{rb}{\vartheta^2}} \sum_{|k-m| \geq \frac{rb}{\vartheta}} \left(\frac{1}{2r\pi} \eta(\vartheta, |k-m|) \|f\|_{L^1(\mathbb{R}^2)} + \frac{1}{2\pi} \epsilon_{-1} \left(f, \frac{\vartheta|k-m|}{r} \right) \right) \\
&\leq \sum_{|k| \leq \frac{rb}{\vartheta^2}} \sum_{l \geq \frac{rb}{\vartheta}} \left(\frac{1}{r\pi} \eta(\vartheta, l) \|f\|_{L^1(\mathbb{R}^2)} + \frac{1}{\pi} \epsilon_{-1} \left(f, \frac{\vartheta l}{r} \right) \right) \\
&\stackrel{(4)}{\leq} \frac{2rb}{\vartheta^2} \left(\frac{1}{\pi r} \eta_1 \left(\vartheta, \frac{rb}{\vartheta} \right) \|f\|_{L^1(\mathbb{R}^2)} + \frac{r}{\pi \vartheta} \epsilon_0(f, b) \right) \\
&\leq \frac{2b}{\pi \vartheta^2} \eta_1 \left(\vartheta, \frac{rb}{\vartheta} \right) \|f\|_{L^1(\mathbb{R}^2)} + \frac{2r^2 b}{\pi \vartheta^3} \epsilon_0(f, b),
\end{aligned}$$

where we have used, $0 < \mu$ and $b > 1$ (see, e.g., [7])

$$\sum_{l \geq b/\mu} \epsilon_d(f, \mu l) \leq \frac{1}{\mu} \epsilon_{d+1}(f, b), \tag{7}$$

for $\mu = \vartheta/r$.

- For the sum S_{12} , we notice that $|k - m| < \vartheta|k|$. Using Lemma 3.5,

$$\begin{aligned}
S_{12} &\leq \sum_{\substack{|k| \geq \frac{rb}{\vartheta^2} \\ |k-m| < \vartheta|k|}} \frac{\vartheta|k|}{2\pi(r^2 - \bar{r}^2)} \eta(\vartheta, |k|) \|f\|_{L^1(\mathbb{R}^2)} \leq \frac{\vartheta}{\pi(r^2 - \bar{r}^2)} \sum_{l \geq \frac{rb}{\vartheta^2}} l \eta(\vartheta, l) \|f\|_{L^1(\mathbb{R}^2)} \\
&\stackrel{(6)}{\leq} \frac{\vartheta}{\pi(r^2 - \bar{r}^2)} \eta_3 \left(\vartheta, \frac{rb}{\vartheta^2} \right) \|f\|_{L^1(\mathbb{R}^2)}.
\end{aligned}$$

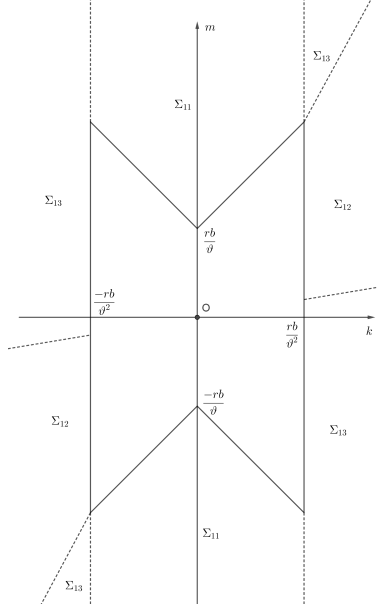


Figure 5: The parts of set $\mathbb{Z}^2 \setminus K$ when we calculate I_1 .

- In Σ_{13} , we get the sum for the m first. Hence, from Lemma 3.4

$$\begin{aligned}
\Sigma_{13} &\leq \sum_{|k| \geq \frac{rb}{\vartheta^2}} \sum_{|k-m| \geq \vartheta|k|} \left(\frac{1}{2\pi r} \eta(\vartheta, |k-m|) \|f\|_{L^1(\mathbb{R}^2)} + \frac{1}{2\pi} \epsilon_{-1} \left(f, \frac{\vartheta|k-m|}{r} \right) \right) \\
&\stackrel{(4),(7)}{\leq} \sum_{|k| \geq \frac{rb}{\vartheta^2}} \left(\frac{1}{2\pi r} \eta_1(\vartheta, \vartheta|k|) \|f\|_{L^1(\mathbb{R}^2)} + \frac{r}{2\pi\vartheta} \epsilon_0 \left(f, \frac{\vartheta^2|k|}{r} \right) \right) \\
&\leq \sum_{l \geq \frac{rb}{\vartheta^2}} \left(\frac{1}{\pi r} \eta_1(\vartheta, l) \|f\|_{L^1(\mathbb{R}^2)} + \frac{r}{\pi\vartheta} \epsilon_0 \left(f, \frac{\vartheta^2 l}{r} \right) \right) \\
&\stackrel{(5),(7)}{\leq} \frac{1}{\pi r} \eta_2 \left(\vartheta, \frac{rb}{\vartheta^2} \right) \|f\|_{L^1(\mathbb{R}^2)} + \frac{r^2}{\pi\vartheta^3} \epsilon_1(f, b).
\end{aligned}$$

PART 2: Estimate S_2

Similarly, we consider the sums S_{21}, S_{22}, S_{23} over the regions

$$\begin{aligned}
\Sigma_{21} &: |k| < \frac{rb}{\vartheta^2} \quad ; \quad |k+m| \geq \frac{rb}{\vartheta} \\
\Sigma_{22} &: |k| \geq \frac{rb}{\vartheta^2} \quad ; \quad |k| > \frac{|k+m|}{\vartheta} \\
\Sigma_{23} &: |k| \geq \frac{rb}{\vartheta^2} \quad ; \quad |k| \leq \frac{|k+m|}{\vartheta}.
\end{aligned}$$

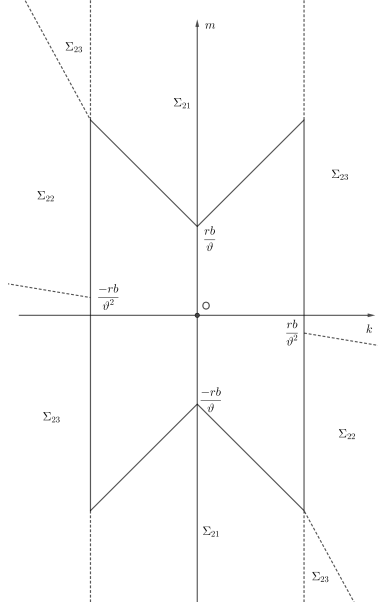


Figure 6: The parts of set $\mathbb{Z}^2 \setminus K$ when we calculate I_2 .

Then,

$$\begin{aligned}
S_{21} &\leq \frac{2b}{\pi\vartheta^2} \eta_1 \left(\vartheta, \frac{rb}{\vartheta} \right) \|f\|_{L^1(\mathbb{R}^2)} + \frac{2r^2b}{\pi\vartheta^3} \epsilon_0(f, b), \\
S_{22} &\leq \frac{\vartheta}{\pi(r^2 - \bar{r}^2)} \eta_3 \left(\vartheta, \frac{rb}{\vartheta^2} \right) \|f\|_{L^1(\mathbb{R}^2)}, \\
S_{23} &\leq \frac{1}{\pi r} \eta_2 \left(\vartheta, \frac{rb}{\vartheta^2} \right) \|f\|_{L^1(\mathbb{R}^2)} + \frac{r^2}{\pi\vartheta^3} \epsilon_1(f, b).
\end{aligned}$$

FINISHING THE PROOF

Combining the estimates in **PART 1** and **PART 2**, we obtain

$$2 \sum_{(k,m) \notin K} |\hat{g}(k, m)| \leq \frac{12}{\pi} \eta^*(\vartheta, rb) \|f\|_{L^1(\mathbb{R}^2)} + \frac{4r^2}{\pi\vartheta^3} (2b+1) \epsilon_1(f, b),$$

where $\eta^*(\vartheta, rb) = \max \left\{ \frac{2b}{\vartheta^2} \eta_1 \left(\vartheta, \frac{rb}{\vartheta} \right); \frac{1}{r} \eta_2 \left(\vartheta, \frac{rb}{\vartheta^2} \right); \frac{\vartheta}{r^2 - \bar{r}^2} \eta_3 \left(\vartheta, \frac{rb}{\vartheta^2} \right) \right\}$

According to Theorem 2.2, we conclude

$$\|S_{W,K}g - g\|_{L^\infty} \leq \frac{12}{\pi} \eta^*(\vartheta, rb) \|f\|_{L^1(\mathbb{R}^2)} + \frac{4r^2}{\pi\vartheta^3} (2b+1) \epsilon_1(f, b).$$

□

3.2 Sampling schemes for $g(\varphi, \psi)$

In this section, we consider two schemes that satisfy the conditions in Theorem 3.1. The first one is the standard scheme, where the sampling locations is the Cartesian product. The second one, more efficient, is an interlaced scheme.

Standard Sampling Scheme

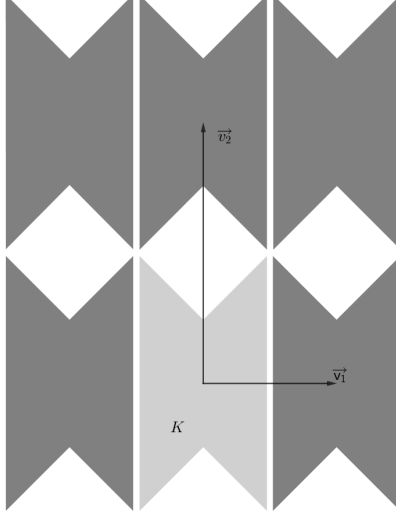


Figure 7: Geometry of the standard sampling scheme.

For the standard sampling, we chose $2\pi W^{-T}$ such that the translates $K + 2\pi W^{-T}m$ are disjoint for any $m \in \mathbb{Z}^2$. From Figure 7 we have a choice

$$2\pi W^{-T} = \begin{pmatrix} \frac{2rb}{\vartheta^2} & 0 \\ 0 & \frac{2rb}{\vartheta} \left(1 + \frac{1}{\vartheta}\right) \end{pmatrix}$$

So that

$$W = \begin{pmatrix} \pi\vartheta^2/rb & 0 \\ 0 & \frac{\pi\vartheta^2}{rb(1+\vartheta)} \end{pmatrix} =: \begin{pmatrix} 2\pi/N_\varphi & 0 \\ 0 & 2\pi/N_\psi \end{pmatrix}$$

We assume that N_φ and N_ψ are integers, otherwise we replace them by $[N_\varphi]$ and $[N_\psi]$.

Assume that f is supported in $|x| < r_0 \leq 1$, so m can be restricted to $|m| < \frac{N_\psi \arcsin(r_0/r)}{2\pi}$. Because the function $g(\varphi, \psi)$ is even in ψ so we only chose $\psi \geq 0$. This yields the standard detector system $g_{k,m} = g(\varphi_k, \psi_m)$, where

$$\begin{aligned} \varphi_k &= \frac{k2\pi}{N_\varphi}, & \text{for } 0 \leq k \leq N_\varphi - 1 \\ \psi_m &= \frac{m2\pi}{N_\psi}, & \text{for } 0 \leq m < \frac{N_\psi \arcsin(r_0/r)}{2\pi}. \end{aligned}$$

The sampling conditions in Theorem 3.1 are satisfied if

$$N_\varphi \geq \frac{2\pi rb}{\vartheta^2}, \quad N_\psi \geq \frac{2rb(1+\vartheta)}{\vartheta^2}.$$

Efficient Sampling Scheme

Again, we need to chose $2\pi W^{-T}$ such that the translates $K + 2\pi W^{-T}m$ are disjoint for any $m \in \mathbb{Z}^2$. Making the following choice (see Fig. 8)

$$2\pi W^{-T} = \begin{pmatrix} \frac{2rb}{\vartheta^2} & -\frac{rb}{\vartheta^2} \\ 0 & \frac{rb}{\vartheta} \left(2 + \frac{1}{\vartheta}\right) \end{pmatrix},$$

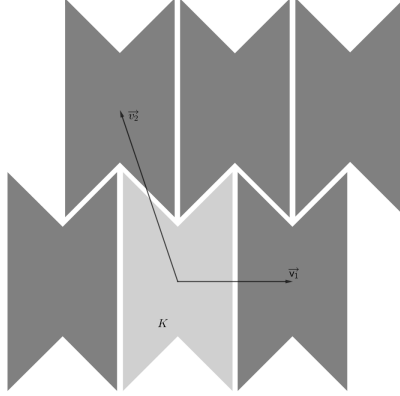


Figure 8: Geometry of efficient sampling scheme.

We obtain

$$W = \begin{pmatrix} \frac{\pi\vartheta^2}{rb} & 0 \\ \frac{\pi\vartheta^2}{rb(1+2\vartheta)} & \frac{2\pi\vartheta^2}{rb(1+2\vartheta)} \end{pmatrix} = \begin{pmatrix} 2\pi/N_\varphi & 0 \\ \pi/N_\psi & 2\pi/N_\psi \end{pmatrix}$$

We obtain the interlaced sampling scheme $(\varphi_k, \psi_{k,m})$ by

$$\varphi_k = \frac{k2\pi}{N_\varphi}, \quad \psi_{k,m} = \frac{\pi(k+2m)}{N_\psi}.$$

Let $l = k + 2m$ then we get the efficient sampling scheme (φ_k, ψ_{kl}) as

$$\begin{aligned} \varphi_k &= \frac{k2\pi}{N_\varphi} & \text{for } 0 \leq k \leq N_\varphi - 1 \\ \alpha_{k,l} &= \frac{\pi l}{N_\psi} & \text{for } k, l \text{ are parity and } 0 \leq l < \frac{N_\psi \arcsin(r_0/r)}{\pi} \end{aligned}$$

which the sampling conditions are

$$N_\varphi \geq \frac{2\pi rb}{\vartheta^2}, \quad N_\psi \geq \frac{rb(1+2\vartheta)}{\vartheta^2}.$$

Taking the limit $\vartheta \rightarrow 1$ we obtain

$$N_\varphi \geq 2\pi rb, \quad N_\psi \geq 3rb.$$

Acknowledgement

Linh Nguyen's research is partially supported by the NSF grants, DMS 1212125 and DMS 1616904.

References

- [1] Moritz Allmaras, David P Darrow, Yulia Hristova, Guido Kanschat, and Peter Kuchment. Detecting small low emission radiating sources. *arXiv preprint arXiv:1012.3373*, 2010.
- [2] Gaik Ambartsoumian. Inversion of the v-line radon transform in a disc and its applications in imaging. *Computers & Mathematics with Applications*, 64(3):260–265, 2012.

- [3] Allan Macleod Cormack. Representation of a function by its line integrals, with some radiological applications. *Journal of applied physics, American Institute of Physics*, 34(9):2722–2727, 1963.
- [4] Roman Basko, Gengsheng L Zeng, and Grant T Gullberg. Analytical reconstruction formula for one-dimensional compton camera. *IEEE Transactions on Nuclear Science*, 44(3):1342–1346, 1997.
- [5] Michael J Cree and Philip J Bones. Towards direct reconstruction from a gamma camera based on compton scattering. *IEEE transactions on medical imaging*, 13(2):398–407, 1994.
- [6] DB Everett, JS Fleming, RW Todd, and JM Nightingale. Gamma-radiation imaging system based on the compton effect. In *Proceedings of the Institution of Electrical Engineers*, volume 124, pages 995–1000. IET, 1977.
- [7] Frank Natterer. The mathematics of computerized tomography. *SIAM*, 2001.
- [8] Natterer, F Sampling in fan beam tomography. *SIAM Journal on Applied Mathematics*, 53(2):358–380, 1993.
- [9] Adel Faridani. A generalized sampling theorem for locally compact abelian groups. *Mathematics of computation*, 63:(207):307–327, 1994.
- [10] Adel Faridani. Fan-beam tomography and sampling theory. *Proceedings of Symposia in Applied Mathematics*, 63:43–66, 2006.
- [11] Adel Faridani. Reconstructing from efficiently sampled data in parallel-beam computed tomography. *Inverse problems and imaging, Pitman Research Notes in Mathematics Series*, 245:68–102, 1991.
- [12] Sigurdur Helgason and S Helgason. *The radon transform*, volume 2. Springer, 1999.
- [13] V P Palamodov. Localization of harmonic decomposition of the Radon transform. *Inverse problems*, 11(5):1025, 1995.
- [14] Lucia Florescu, John C Schotland, and Vadim A Markel. Single-scattering optical tomography. *Physical Review E*, 79(3):036607, 2009.
- [15] Rim Gouia-Zarrad and Gaik Ambartsoumian. Exact inversion of the conical radon transform with a fixed opening angle. *Inverse Problems*, 30(4):045007, 2014.
- [16] Fatma Terzioglu. Some inversion formulas for the cone transform. *Inverse Problems*, 31(11):115010, 2015.
- [17] Markus Haltmeier. Exact reconstruction formulas for a radon transform over cones. *Inverse Problems*, 30(3):035001, 2014.
- [18] Haltmeier, Markus. Sampling conditions for the circular radon transform. *IEEE Transactions on Image Processing*, 25.6 (2016): 2910–2919.
- [19] Yulia Hristova. Inversion of a v-line transform arising in emission tomography. *Journal of Coupled Systems and Multiscale Dynamics*, 3(3):272–277, 2015.
- [20] Chang-Yeol Jung and Sunghwan Moon. Inversion formulas for cone transforms arising in application of compton cameras. *Inverse Problems*, 31(1):015006, 2015.
- [21] Peter Kuchment and Fatma Terzioglu. Three-dimensional image reconstruction from compton camera data. *SIAM Journal on Imaging Sciences*, 9(4):1708–1725, 2016.
- [22] Sunghwan Moon and Markus Haltmeier. Analytic inversion of a conical radon transform arising in application of compton cameras on the cylinder. *SIAM Journal on imaging sciences*, 10(2):535–557, 2017.
- [23] Marcela Morvidone, Mai Khuong Nguyen, Tuong T Truong, and Habib Zaidi. On the v-line radon transform and its imaging applications. *Journal of Biomedical Imaging*, 2010:11, 2010.

- [24] Mai K Nguyen, Tuong T Truong, and Pierre Grangeat. Radon transforms on a class of cones with fixed axis direction. *Journal of Physics A: Mathematical and General*, 38(37):8003, 2005.
- [25] Daniela Schiefeneder and Markus Haltmeier. The radon transform over cones with vertices on the sphere and orthogonal axes. *SIAM Journal on Applied Mathematics*, 77(4):1335–1351, 2017.
- [26] Keeve M. Siegel. An inequality involving Bessel functions of argument nearly equal to their order. *Proceedings of the American Mathematical Society*, 4(6):858–859, 1953.
- [27] Manbir Singh. An electronically collimated gamma camera for single photon emission computed tomography. part i: Theoretical considerations and design criteria. *Medical Physics*, 10(4):421–427, 1983.
- [28] Stefanov, Plamen. Semiclassical sampling and discretization of certain linear inverse problems. *arXiv preprint arXiv:1811.01240*, 2018.
- [29] Terras, Audrey. Harmonic Analysis on Symmetric Spaces and Applications I. Springer Science & Business Media, 2012.
- [30] Tuong T Truong and Mai K Nguyen. On new v-line radon transforms in \mathbb{R}^2 and their inversion. *Journal of Physics A: Mathematical and Theoretical*, 44(7):075206, 2011.